



*Citation for published version:*

Hassanpour Amiri, M, Sharifi Dehsari, H & Asadi, K 2022, 'Magnetoelectric coupling coefficient in multiferroic capacitors: Fact vs Artifacts', *Journal of Applied Physics*, vol. 132, no. 16, 164102.  
<https://doi.org/10.1063/5.0107365>

*DOI:*

[10.1063/5.0107365](https://doi.org/10.1063/5.0107365)

*Publication date:*

2022

*Document Version*

Peer reviewed version

[Link to publication](#)

This article may be downloaded for personal use only. Any other use requires prior permission of the author and AIP Publishing. The following article appeared in Morteza Hassanpour Amiri, Hamed Sharifi Dehsari, Kamal Asadi; Magnetoelectric coupling coefficient in multiferroic capacitors: Fact vs Artifacts. *J. Appl. Phys.* 28 October 2022; 132 (16): 164102. <https://doi.org/10.1063/5.0107365> and may be found at <https://pubs.aip.org/aip/jap/article-abstract/132/16/164102/2837607/Magnetoelectric-coupling-coefficient-in?redirectedFrom=fulltext>

**University of Bath**

## **Alternative formats**

If you require this document in an alternative format, please contact:  
[openaccess@bath.ac.uk](mailto:openaccess@bath.ac.uk)

### **General rights**

Copyright and moral rights for the publications made accessible in the public portal are retained by the authors and/or other copyright owners and it is a condition of accessing publications that users recognise and abide by the legal requirements associated with these rights.

### **Take down policy**

If you believe that this document breaches copyright please contact us providing details, and we will remove access to the work immediately and investigate your claim.

## Magnetoelectric coupling coefficient in multiferroic capacitors; fact versus artefacts

Morteza Hassanpour Amiri<sup>1</sup>, Hamed Sharifi Dehsari<sup>1</sup>, Kamal Asadi<sup>1,2,3\*</sup>

<sup>1</sup> Max Planck Institute for Polymer Research, Ackermannweg 10, 55128, Mainz, Germany

<sup>2</sup> Department of Physics, University of Bath, Claverton Down, BA2 7AY, Bath, United Kingdom.

<sup>3</sup> Centre for Therapeutic innovations, University of Bath, Bath, United Kingdom.

\* Corresponding author; Email: ka787@bath.ac.uk

### Abstract:

Multiferroic materials are characterized by their magnetoelectric coupling coefficient, which can be obtained using a lock-in amplifier by measuring the voltage developed across a multiferroic capacitor in a time-variable magnetic field,  $H_{ac}\cos(\omega t)$ , where  $H_{ac}$  and  $\omega$  are the amplitude and frequency of the applied magnetic field. The measurement method, despite its simplicity, is subject to various parasitic effects, such as magnetic induction, which leads to significant over-estimation of the actual magnetoelectric response. This manuscript outlines the measurement theory for a multiferroic capacitor using the lock-in technique. It is demonstrated that the inductive contribution has linear proportionality with  $H_{ac}$ ,  $\omega$ , and  $H_{ac}\omega$ . It is shown that the true magnetoelectric coupling response is retrieved from the real component of the lock-in signal. Using a polymer-nanoparticle multiferroic composite, the internal consistency of the proposed measurement method is experimentally demonstrated, and it is shown that the actual multiferroic signal can be retrieved using the lock-in technique by removing the magnetic induction contribution from the signal. It is observed that the magnetoelectric voltage shows only a linear dependence with  $H_{ac}$ , and a saturating behavior with  $\omega$ , and  $H_{ac}\omega$ . Furthermore, a measurement protocol for reliable reporting of magnetoelectric coupling coefficient has been provided.

## Introduction

Multiferroic materials have emerged as promising multifunctional materials suitable for various applications, from information storage and neuromorphic computing to magnetic field sensors. Multiferroics, being a single-phase, bimorph laminate or (nano)composite, have ignited an immense research interest due to the existence of the magnetoelectric coupling between the magnetic and ferroelectric properties of the material.<sup>1-7</sup> The magnetoelectric coupling coefficient,  $\alpha_{ME}$ , characterizes the strength of magnetoelectric interaction, and is evaluated through two methods; I) direct  $\alpha_{ME}$ , where a magnetic field is applied, and the induced changes in the electric field are measured, or II) converse  $\alpha_{ME}$  where an electric field is applied across the sample, and the induced magnetization (or changes in the magnetic field) is measured.<sup>8-10</sup>

Measurement of the direct  $\alpha_{ME}$ , i.e., magnetically induced electric field in a multiferroic capacitor has emerged as a relatively straightforward method for the evaluation of the  $\alpha_{ME}$  coupling coefficient. The direct  $\alpha_{ME}$  can be expressed as:

$$\alpha_{ME} = \frac{\partial E}{\partial H_{ac}} = \frac{\partial V_{ME}}{t \partial H_{ac}} \text{ (in mV Oe}^{-1}\text{cm}^{-1}\text{)} \quad (1)$$

where  $t$  is the thickness of the multiferroic film and  $V_{ME}$  is the voltage induced by a time-varying (AC) magnetic field,  $H_{ac}$ , across a capacitor. The lock-in technique is a widely used method that quantitatively measures  $V_{ME}$  from which  $\alpha_{ME}$  is easily calculated.<sup>11</sup> A schematic of the measurement setup is presented in Figure 1.

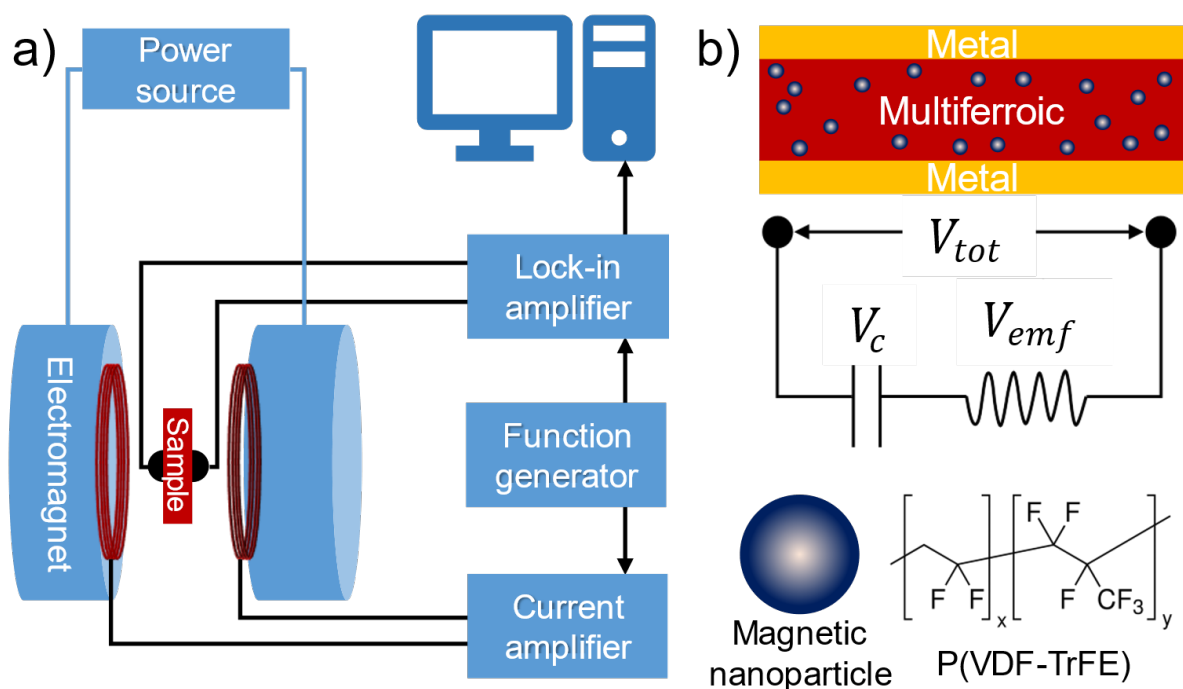


**Figure 1.** a) A schematic of a typical lock-in measurement setup. b) Schematic of the magnetic nanoparticle/ferroelectric polymer composite multiferroic capacitor employed for the experimental verification of the proposed method (top), the corresponding equivalent LC circuit of the multiferroic capacitor (middle), and the schematic representation of  $\text{Co}_{0.7}\text{Fe}_{2.3}\text{O}_4$  nanoparticles and P(VDF-TrFE) piezoelectric polymer (bottom).

In the lock-in measurement technique, a small alternating magnetic field  $H_{ac}$  (usually superimposed on a dc magnetic field,  $H_{dc}$ ) is applied to the sample. The sample is typically a capacitor, where the multiferroic material is sandwiched between two metallic electrodes. The  $\alpha_{ME}$  coefficient for the multiferroic is obtained by monitoring the voltage (in the open-circuit condition) across the capacitor using a lock-in amplifier whose frequency is locked with the frequency of the applied  $H_{ac}$ . The lock-in synchronization eliminates all possible parasitic voltages at frequencies other than the locked frequency. Under ideal conditions, when there is no leakage current through the samples, lock-in records  $V_{ME}$ . However, additional voltages resulting from electromagnetic induction must be considered when measuring the  $\alpha_{ME}$  coefficient. Due to the magnetic induction, the multiferroic capacitor subjected to a variable magnetic flux is the source of an electromotive force (*emf*). The *emf* voltage usually can be comparable to, or even larger than the  $V_{ME}$  for small samples or samples with weak  $\alpha_{ME}$  coefficients. Thus, removing the *emf* contribution due to magnetic induction from the signal recorded by the lock-in amplifier is crucial. Otherwise, calculating the  $\alpha_{ME}$  coefficient from the recorded lock-in voltage amplitude can significantly over-estimate the actual coupling coefficient. Currently, there is no method to remove the *emf* contribution.

Here we present the analysis of the lock-in measurement theory and present an experimentally verified method to record the magnetoelectric signal,  $V_{ME}$ , and accurately evaluate  $\alpha_{ME}$  for multiferroic capacitors. The modified protocol enables identifying and removal of the parasitic signals due to *emf*, and is very beneficial for evaluation of samples with a weak magnetoelectric signal,  $V_{ME}$ .

## Results and discussions

The lock-in amplifier reports two parameters: 1) A voltage amplitude,  $V$ , and 2) a phase angle, defined as  $\theta$ .<sup>12</sup> In the literature,  $V$  is commonly reported as the ME coupling response. In contrast, the phase angle of the lock-in signal is surprisingly usually overlooked. To understand the role of each lock-in parameter, let us first establish the principles of the lock-in measurement technique and decipher the meaning of each parameter.

The simplest equivalent circuit of a multiferroic capacitor which includes the distributed capacitors and inductors in the signal path, is an LC circuit, thus a voltage divider, as shown in Figure 1b. The lock-in amplifier measures  $V_{tot}$ , which is:

$$V_{tot} = V_c + V_L \quad (2)$$

where  $V_c$  and  $V_L$  are the voltages across the capacitor and inductor, respectively. Now, a time-varying magnetic field ( $H(t) = H_{ac} \cos(\omega t)$ ) is applied to the multiferroic capacitor via the Helmholtz coil. We will use the Euler representation of the  $H(t)$  to simplify the derivations:

$$H(t) = \frac{H_{ac}}{2} (e^{i\omega t} + e^{-i\omega t}) \quad (3)$$

The applied magnetic field induces voltage via magnetic induction in the inductor:<sup>13</sup>

$$V_L = -\frac{d\varphi}{dt} = -\frac{d(B.A)}{dt} = -A \frac{d(\mu H)}{dt} = -\mu A \frac{dH}{dt} = -\mu A \frac{H_{ac}}{2} i\omega (e^{i\omega t} - e^{-i\omega t}) \quad (4)$$

where  $A$  is the area of the capacitor plates,  $\mu$  is the permeability of the multiferroic material. Note that  $V_L$  has a negative sign and oscillates with the same frequency as the applied ac-magnetic field but with a 90° phase difference.

The application  $H_{ac}$  induces a voltage across the capacitor due to the magnetoelectric coupling in the multiferroic material:<sup>14</sup>

$$V_C = \frac{V_{ME}}{2}(e^{i\omega_c t} + e^{-i\omega_c t}) \quad (5)$$

where  $V_{ME}$  is the magnetically induced magnetoelectric voltage, as defined earlier. Note that in an ideal case,  $V_C$ , oscillates with the same frequency  $\omega$  as the applied  $H(t)$ , and is in phase with it (or  $180^\circ$  out of phase depending on the sign of the piezoelectric  $d_{33}$  constant). Here, for the sake of generality, it is assumed that  $V_C$  oscillated at a different frequency  $\omega_c$ . Hence  $V_{tot}$  is:

$$V_{tot} = V_C + V_L = \frac{V_{ME}}{2}(e^{i\omega_c t} + e^{-i\omega_c t}) - \mu A \frac{H_{ac}}{2} i\omega (e^{i\omega t} - e^{-i\omega t}) \quad (6)$$

The lock-in amplifier processes the incoming  $V_{tot}$  signal via the dual-phase down-mixing, which is mathematically expressed as a multiplication of the incoming signal with the complex reference signal, fed via the function generator, which is of the form:

$$v_r(t) = V_r \cos(\omega_r t) = e^{i\omega_r t} + e^{-i\omega_r t} \quad (7)$$

where for simplicity of the calculations is assumed that  $|V_r| = 2$  so that the Euler representation gives  $v_r(t) = \cos(\omega_r t)$ , which has the conventional form used in a lock-in amplifier.<sup>15</sup> The complex voltage signal that enters the lock-in amplifier is  $V_{tot}(t) \times v_r(t)$  with signal components at the sum and the difference between the signal and reference frequencies, which can be written as:

$$Z(t) = V_{tot}(t) \times v_r(t) = \frac{V_{ME}}{2} (e^{i(\omega_r+\omega_c)t} + e^{i(\omega_r-\omega_c)t} + e^{-i(\omega_r-\omega_c)t} + e^{-i(\omega_r+\omega_c)t}) - \mu A \frac{H_{ac}}{2} i\omega (e^{i(\omega_r+\omega)t} + e^{i(\omega_r-\omega)t} + e^{-i(\omega_r+\omega)t} + e^{-i(\omega_r-\omega)t}) \quad (8)$$

The demodulation of the signal by the lock-in implies that signals with  $(\omega_c + \omega_r)$  are filtered.

By definition, the lock-In technique dictates  $\omega_c \approx \omega_r$ . Hence  $Z$  can be stated as

$$Z = X + iY = V_{ME} - i\omega H_{ac} \mu A \quad (9)$$

with  $X = V_{ME}$  is the pure magnetoelectric contribution and  $Y = -i\omega H_{ac} \mu A$  is purely due to magnetic induction. Equation 9 is the demodulated signal produced by the lock-in amplifier. The lock-in amplifier, however, usually produces an amplitude  $V$  and a phase  $\theta$  of the signal in the form:<sup>15</sup>

$$Z = V e^{i\theta} \text{ where } V = \sqrt{X^2 + Y^2}, \text{ and } \theta = \arctan\left(\frac{Y}{X}\right) \quad (10)$$

with the absolute value  $|Z| = V$  given as the amplitude of the signals and  $\theta$  given by the phase of the input signal relative to the reference signal. The value for  $\theta$  requires close attention; values close to  $\pm 90^\circ$  indicate the dominance of the imaginary component or the inductive contribution to the lock-in signal. In contrast, a value approaching zero indicates the dominance of the magnetoelectric contribution. Any values for  $\theta$  between these two limits indicate that the signal is a mixture of magnetoelectric and inductive responses. Note that the magnetic inductive y-component of the signal is always 90 degrees out of phase with the reference signal. According to Lenz's law, the inductive phase cannot change the frequency and thus will have the same frequency as the AC magnetic field.

The mathematics that outlines the measurement principles indicates that under no circumstances the value of  $V$  alone should be taken as the amplitude of the magnetoelectric signal. The correct value that should be assigned to the magnetoelectric response of the device is  $V \cos \theta$ , which is the  $X$  component of the signal amplitude measured by the lock-in amplifier. The imaginary part of the signal due to the inductive contribution has linear dependencies with  $\omega$ ,  $H_{ac}$  and  $\omega H_{ac}$  as indicated in Equation 9. Depending on the applied  $\omega$  and  $H_{ac}$  the inductive contribution can become very large, which, if extra caution is not taken, will lead to reporting unrealistically large values for the magnetoelectric coupling coefficient  $\alpha_{ME}$ . The dependencies of  $V_{ME}$  to both  $\omega$  and  $H_{ac}$  cannot be determined *a priori* and are determined experimentally. For magnetoelectric bimorph composites or

nanocomposites, it is expected that  $V_{ME}$  shows frequency dependence because it originates from the strain transfer from the magnetic to the piezoelectric phase, whose piezoelectric coefficient and dielectric constant nonlinearly depend on the mechanical excitation frequency.

Having established the basics of the lock-in measurement, let us now experimentally examine these findings. To do so, multiferroic capacitors were fabricated from nanocomposites of  $\text{Co}_{0.7}\text{Fe}_{2.3}\text{O}_4$  nanoparticles and piezoelectric polymer poly(vinylidene fluoride-co-trifluoroethylene), P(VDF-TrFE). The nanoparticles were synthesized using thermal decomposition methods.<sup>16</sup> The reaction conditions were controlled to produce particles with spherical geometry and uniform size distribution of  $13 \pm 2$  nm (determined using tunneling electron microscope, TEM). Details of nanoparticle synthesis have been reported previously.<sup>19</sup> The resulting nanoparticles were mixed with P(VDF-TrFE) and processed into a film using a bar coater from the solution phase. Details of the capacitor fabrication have been reported previously.<sup>17</sup> The capacitors were fabricated using Au bottom and top electrodes that were evaporated through shadow masks using thermal evaporation. Schematics of the multiferroic capacitor and the chemical structure of the compounds are given in Figure 1b. All magnetoelectric measurements were performed at room temperature under He gas atmosphere. Before commencing the lock-in measurement, the nanoparticles were magnetized by applying a large dc magnetic field,  $H_{ac}$ , of 1 T to the capacitors, and the P(VDF-TrFE) piezoelectric matrix was poled by applying a dc electric field of 80 MV/m.

Figure 2a displays a typical example of the measurement for  $X$ ,  $Y$  and  $V$  for a fixed  $H_{ac} = 0.5$  T and  $H_{ac}$  values of 0.6 mT. The imaginary component,  $Y$ , is negative and has a perfectly linear relationship with the applied frequency (as predicted by Equation 9). The magnetoelectric voltage,  $X$ , component of the signal shows starkly different behavior with a much weaker frequency dependence that tends to saturate at higher frequencies, in sharp contrast to the  $Y$  component that linearly increases with frequency. The frequency response of  $V_{ME}$  stems from the frequency dependence of the piezoelectric properties of the polymer matrix. It is interesting to note that at low frequencies  $V_{ME} > |V_{emf}|$ , whereas at higher frequencies  $V_{ME} < |V_{emf}|$ . As shown in Figure 2a, reporting the amplitude of the lock-in amplifier signal  $V$  instead of its real component  $X$ , leads to a substantially over-estimated voltage (consequently artificially inflated  $\alpha_{ME}$  coupling coefficients) due to the significant contribution of magnetic induction. For example, the  $\alpha_{ME}$  obtained from the  $V$  value at 10 kHz in Figure 2a reaches as high as 2300 mV/Oe.cm, which is substantially larger than what is obtained from actual magnetoelectric contribution, which is 750 mV/Oe.cm. Note that  $Y$  should also exhibit a linear dependency to  $H_{ac}$  according to Equation 9. Interestingly,  $V_{ME}$  also, linearly depends on  $H_{ac}$  within the experimental boundary conditions. Consequently, the linear dependence on  $H_{ac}$  is also reflected in the amplitude of the lock-in amplifier signal,  $V$ . Hence, linear  $H_{ac}$  dependence of the lock-in amplifier signals cannot be distinctively considered as a signature of a magnetoelectric signal.

To check the validity and internal consistency of the mathematical analysis presented above, we have plotted both  $X$  and  $Y$  measured at various frequencies and  $H_{ac}$  values as a function of  $\omega H_{ac}$  in Figure 3. All the measured  $Y$  values at different  $H_{ac}$  and  $\omega$  show a linear dependence with  $\omega H_{ac}$  and collapse onto a universal curve, Figure 3a, as expected from Equation 9. The linear fit through data produces a line with  $R^2=99.6\%$ , with a gradient of  $4 \mu\text{V.s/T}$ . In sharp contrast, the  $X$  (or  $V_{ME}$ ) component of the lock-in signal does not yield any scaling, Figure 3b, as the values preserve their saturating trend with increasing  $\omega H_{ac}$ . The perfect consistency between measured  $Y$  and what is predicted by Equation 9 indicates that the analysis of the measurement protocol provided here is entirely consistent. Therefore, it is a correct practice to record the  $X$  component of the lock-in amplifier amplitude as the “true” multiferroic coupling coefficient. The  $X$  and  $Y$  components of the demodulated signal from the lock-in amplifier can be unambiguously assigned to  $V_{ME}$  and the magnetic induction, respectively.

## Conclusion

Lock-in techniques can unambiguously measure the voltage due to magnetoelectric coupling in multiferroic capacitors in a magnetic field. The real and imaginary components of the lock-in signal can be assigned to the voltage due to multiferroic coupling and magnetic induction, respectively. In the analysis presented, it is assumed that the capacitor is loss-free and no leakage current passes through the device. The presence of the leakage current reduces the contribution due to magnetoelectric coupling and enhances the contribution of the inductive component in the lock-in amplitude signal. Based on the analysis presented:

I) The inductive contribution due to emf has a  $\pm 90^\circ$  phase difference with the applied  $H_{ac}$ . If the phase difference between the lock-in amplifier amplitude with  $H_{ac}$  is neither  $0^\circ$  (or  $180^\circ$ ) nor  $\pm 90^\circ$ , the measured signal is a mixture of the voltages due to magnetoelectric coupling and magnetic induction, *emf*.

II) Both magnetoelectric and *emf* signals show a linear dependence on  $H_{ac}$ . For self-biased composites, the signals do not show (or exhibit just a weak) dependence on  $H_{dc}$ . Otherwise, the magnetoelectric coupling coefficient should depend on the dc magnetic field. It has been experimentally demonstrated that  $V_{ME}$  changes with  $H_{dc}$  and maximize at a certain value.<sup>12</sup> The component due to *emf* does not depend on  $H_{dc}$ .

III) The voltage due to magnetic induction,  $V_{emf}$ , varies linearly with  $\omega H_{ac}$  of the applied field. The gradient of the linear fit is equivalent to the device area multiplied by the permeability of the multiferroic. Hence the inductive component can be used to indirectly evaluate the effective permeability of the multiferroic material, particularly in the case of (nano)composites.

IV) The  $\omega H_{ac}$  dependence of  $V_{ME}$  is different from  $V_{emf}$  and should generally exhibit a nonlinear behavior with the applied frequency. It is expected that  $V_{ME}$  (concomitantly the  $\alpha_{ME}$ ) follows the frequency dependence of the dielectric constant and  $d_{33}$  of the piezoelectric phase for bimorph and particulate multiferroic composites.

V) The contribution of  $V_{emf}$  can be minimized by positioning the sample such that the applied  $H(t)$  is parallel to the sample plane, hence minimizing  $B \cdot A$  contribution in equation 4, and thereby reducing the *emf* signal.

VI) Another issue that deserves attention is the eddy current induced in metal electrodes. The eddy current is mainly responsible for the parasitic voltage induced across any multiferroic device, particularly at low frequencies and can become a point of concern, particularly for thin-film devices, small area devices, or multiferroic materials with low  $\alpha_{ME}$  coefficients. It has been experimentally demonstrated that for  $H_{dc} \parallel H_{ac}$  configuration eddy current is zero, whereas for the case  $H_{dc} \perp H_{ac}$ , the current is maximum and increases linearly with the applied  $H_{ac}$ .<sup>18</sup> Hence to avoid any contribution from eddy current, the measurement setup should adopt a parallel configuration of  $H_{dc} \parallel H_{ac}$  or a parallel configuration of internal magnetization of the sample with the applied  $H_{ac}$ . We note that other noise sources include thermal noise and vibration or acoustic noises, which cause parasitic currents due to the pyroelectric and piezoelectric effects, respectively.

VII) The measurement theory developed here is generic and material independent thereby applicable to all types of multiferroic capacitors including single phase multiferroic materials or layered heterostructure multiferroics materials such as those fabricated by sandwiching of ferroelectric/ferromagnetic layers. However, for multiferroic capacitors with a very strong magnetoelectric coupling coefficient, such as sandwiched bimorph structures, the voltage due to

magnetoelectric coupling is much larger than the *emf* contribution. Hence, the reported voltages for these systems, although very close to the actual magnetoelectric response of the system, still contains a fraction of the inductive contribution. It is suggested that future works should report both real and imaginary (or amplitude and phase) components of the lock-in signal, and the real (or  $V\cos\theta$ ) component should be reported as the actual multiferroic response.

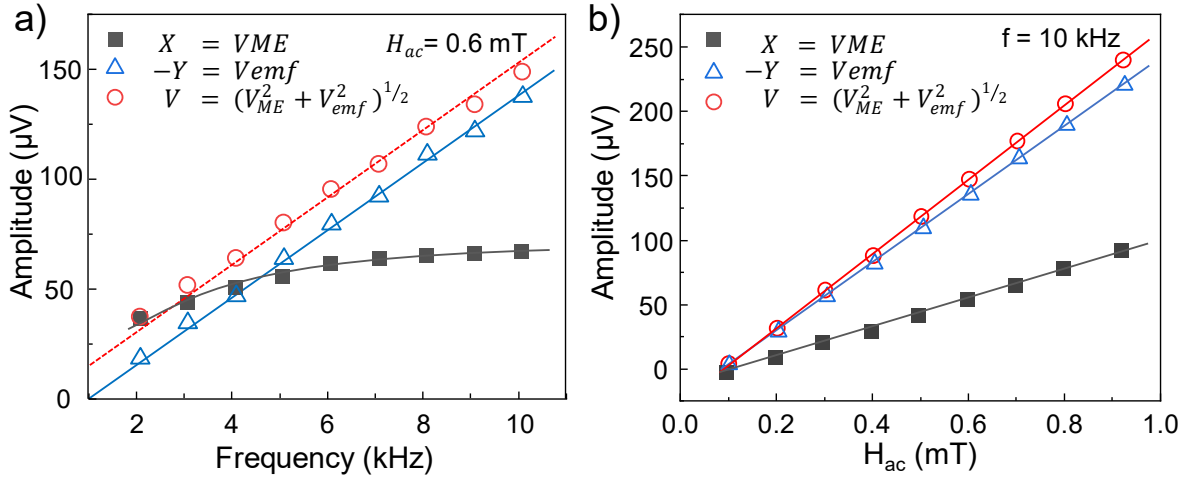


**Figure 2.** a) Frequency and amplitude response of the measured voltage by the lock-in amplifier at two different  $H_{ac}$ . The Y component shows perfect linearity with frequency, as expected from theory. The X component shows a saturating trend with increasing frequency. The correct value for ME voltage is the X component. Applied  $H_{ac}$  is 0.6 T. Note that the amplitudes are different for different  $H_{ac}$  values. b) Dependence of the real part, imaginary part and magnitude of the voltage signal on the applied  $H_{ac}$  at a fixed frequency.

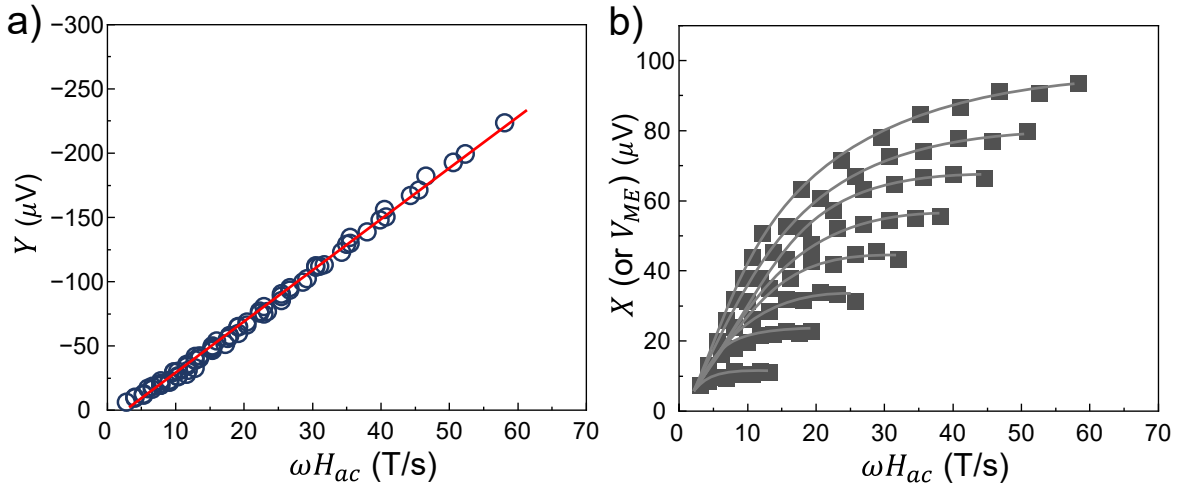


**Figure 3.** Internal consistency check of the measurement protocol. a) Collapse of the Y components of the demodulated signals with  $\omega H_{ac}$  indicating its inductive nature. The solid line is a linear fit to the data. b) The same plot obtained for the X component of the demodulated signal, which is the magnetoelectric coupling voltage,  $V_{ME}$ . The lines are provided as a guide to the eye.





## References

1. Y. Cheng, B. Peng, Z. Hu, Z. Zhou and M. Liu, "Recent development and status of magnetoelectric materials and devices" *Phys. Lett. A* 382, 3018-3025 (2018).
2. T. Sadat, D. Faurie, P. Godard, D. Thiaudière, P. Renault and F. Zighem, "90° ferroelectric domain switching effect on interfacial strain mediated magnetoelectric coupling", *J. Phys. D: Appl. Phys.* 53(15), 145001 (2020).
3. N. A. Spaldin and R. Ramesh, "Advances in magnetoelectric multiferroics", *Nat. Mater.* 18, 203-212 (2019).
4. S. Manipatruni, D. E. Nikonov and I. A. Young, "Beyond CMOS computing with spin and polarization", *Nat. Phys.* 14, 338-343(2018).
5. S. Khizroev, "Technobiology's Enabler: The Magnetoelectric Nanoparticle", *Cold Spring Harb. Perspect. Med.* 9, a034207 (2019).
6. J. Wang, J. B. Neaton, H. Zheng, V. Nagarajan, S. B. Ogale, B. Liu, D. Viehland, V. Vaithyanathan, D. G. Schlom, U. V. Waghmare, N. A. Spaldin, K. M. Rabe, M. Wuttig and R. Ramesh, *Science* 299, 1719-1722 (2003).
7. T. Kimura, T. Goto, H. Shintani, K. Ishizaka, T. -H., Arima and Y. Tokura, *Nature* 426, 55-58 (2003).
8. R. Ramesh, N. Spaldin, *Nat. Mater.* 6, 21 (2007).
9. Y. L. Huang, D. Nikonov, C. Addiego, R. V. Chopdekar, B. Prasad, L. Zhang, J. Chatterjee, H. Liu, A. Farhan, Y. Chu, M. Yang, M. Ramesh, Z. Q. Qiu, B. D. Huey, C. Lin, T. Gosavi, J. Iniguez, J. Bokor, X. Pan, I. Young, L. W. Martin, R. Ramesh *Nat Commun.* 11, 2836 (2020).
10. G. V. Duong, R. Groessinger, M. Schoenhardt, D. Bueno-Basques, *J. Magn. Magn. Mater.* 316 390-393 (2007).
11. M. M. Vopson, Y. K. Fetisov, G. Caruntu, G. Srinivasan *Materials* 10, 963 (2017).
12. J. Ma, L. Song, C. Liu, C. Xin in *Magnetoelectric Polymer-Based Composites* (Ed. S. Lanceros-Méndez, P. Martins), Wiley-VCH, 13, (2017).
13. D. Griffiths, *Introduction To Electrodynamics*, 4th Edition, (Cambridge University Press, 2017)
14. M. M. Kumar, M. Srinivas, S. V. Suryanarayana, G. S. Kumar, T. Bhimasankaram, *Bull. Mater. Sci.* 21, 251 (1998).
15. See for example: "[https://www.zhinst.com/sites/default/files/li\\_primer/zi\\_whitepaper\\_principles\\_of\\_lock-in\\_detection.pdf](https://www.zhinst.com/sites/default/files/li_primer/zi_whitepaper_principles_of_lock-in_detection.pdf)" (accessed June 2022).
16. H. Sharifi Dehsari, M. Heidari, A. H. Ribeiro, W. Tremel, G. Jakob, D. Donadio, R. Potestio, K. Asadi *Chemistry of Materials*, 29 (22), 9648-9656 (2017).

17. H. Sharifi Dehsari, M. Kumar, A. Saad, M. Hassanpour Amiri, C. Yan, S. Anwar, G. Glasser, K. Asadi, *ACS Appl. Nano. Mater.* 1, 6247 (2018).

18. B. Guiffard, D. Guyomar, L. Garbuio, R. Belouadah, J. Zhang, P. J. Cottinet, *Appl. Phys. Lett.* 96, 044105 (2010).

19. H. Sharifi Dehsari, K. Asadi, *J. Phys. Chem. C* 122, 29106 (2018).